Microscopic calculations of transport properties of neutron matter

Omar Benhar,[1,2,*] Artur Polls,[3] Marco Valli,[1,2] and Isaac Vidaña[4]
[1]*INFN, Sezione di Roma, I-00185 Roma, Italy*
[2]*Dipartimento di Fisica, Università "La Sapienza", I-00185 Roma, Italy*
[3]*Departament d'Estructura i Constituents de la Matèria, E-08028 Barcelona, Spain*
[4]*Centro de Física Computacional, Department of Physics, University of Coimbra, P-3004-516 Coimbra, Portugal*
(Received 26 November 2009; published 8 February 2010)

We discuss the results of calculations of the shear viscosity and thermal conductivity of pure neutron matter, carried out within the Landau-Abrikosov-Khalatnikov formalism. The probability of neutron-neutron collisions in the nuclear medium has been obtained from a realistic potential, using both the correlated basis function and the G-matrix approach. The results of our work indicate that medium modifications of nucleon-nucleon scattering are large, their inclusion leading to a dramatic enhancement of the transport coefficients. On the other hand, the results obtained from the two theoretical schemes appear to be in fairly good agreement.

DOI: 10.1103/PhysRevC.81.024305 PACS number(s): 21.65.−f, 26.60.−c, 97.60.Jd

I. INTRODUCTION

The knowledge of transport properties of neutron matter is relevant to the understanding of a variety of neutron star properties. Viscosity plays a crucial role in determining the onset of the gravitational-wave-driven instability, associated with the excitation of r-modes, in rapidly rotating stars [1], while thermal conductivity is one of the factors determining neutron star cooling [2].

Unlike the equation of state (EOS), which is generally obtained from realistic dynamical models, strongly constrained from nuclear systematics and nucleon-nucleon scattering data, the nonequilibrium properties of neutron star matter are often studied using oversimplified models of the nucleon-nucleon (NN) interaction.

The main difficulty involved in calculation of transport coefficients within the formalism originally developed by Abrikosov and Khalatnikov (AK) [3], based on the Landau theory of normal Fermi liquids [4], is the determination of the NN collision probability in the nuclear medium. Most studies of the transport properties of neutron star matter have circumvented this problem, neglecting medium modifications of the NN cross sections altogether and using the measured NN scattering phase shifts to construct the collision probability [5–7].

Nuclear many-body theory (NMBT) provides a consistent framework to obtain the in-medium NN cross section and the transport coefficients of nuclear matter from realistic NN potentials, using either the G-matrix [8] or the correlated basis function (CBF) [10] formalism. In both approaches one can define a well-behaved effective interaction, suitable for use in perturbation theory in the Fermi gas basis and allowing for a *consistent* treatment of equilibrium and nonequilibrium properties [8–10].

In this paper we discuss the results of calculations of the shear viscosity and thermal conductivity of pure neutron matter, carried out using the CBF and G-matrix effective interactions.

In Sec. II, after outlining the elements of NMBT, we analyze the main features of the CBF and G-matrix effective interactions, while Sec. III is devoted to discussion of the in-medium NN cross section in the kinematical setup relevant to the calculation of transport coefficients. The main features of the AK formalism are reviewed in Sec. IV, where we also present the results of numerical calculations. Finally, in Sec. V we summarize our findings and state the conclusions.

II. EFFECTIVE INTERACTIONS IN NUCLEAR MANY-BODY THEORY

NMBT is based on the tenet that nuclei can be described in terms of pointlike nucleons, whose dynamics are dictated by the Hamiltonian,

$$H = \sum_i \frac{\mathbf{k}_i^2}{2m} + \sum_{j>i} v_{ij} + \sum_{k>j>i} V_{ijk}, \tag{1}$$

where $\mathbf{k}_i$ and m are the momentum of the ith nucleon and its mass, respectively.

The NN potential v_{ij} reduces to the Yukawa one-pion exchange potential at large distances, while its behavior at short and intermediate range is determined by a fit of deuteron properties and NN scattering phase shifts. The state-of-the-art NN parametrization referred to as the Argonne v_{18} potential [11] is written in the form

$$v_{ij} = \sum_{n=1}^{18} v_n(r_{ij}) O_{ij}^n. \tag{2}$$

In Eq. (2)

$$O_{ij}^{n\leqslant 6} = [1, (\boldsymbol{\sigma}_i \cdot \boldsymbol{\sigma}_j), S_{ij}] \otimes [1, (\boldsymbol{\tau}_i \cdot \boldsymbol{\tau}_j)], \tag{3}$$

where $\boldsymbol{\sigma}_i$ and $\boldsymbol{\tau}_i$ are Pauli matrices acting in spin and isospin space, respectively, and

$$S_{ij} = \frac{3}{r_{ij}^2}(\boldsymbol{\sigma}_i \cdot \mathbf{r}_{ij})(\boldsymbol{\sigma}_j \cdot \mathbf{r}_{ij}) - (\boldsymbol{\sigma}_i \cdot \boldsymbol{\sigma}_j). \tag{4}$$

The operators corresponding to $n = 7, \ldots, 14$ are associated with the nonstatic components of the NN interaction, while

*benhar@roma1.infn.it

those corresponding to $n = 15, \ldots, 18$ account for small charge symmetry violations. Being fit to the full Nijmegen phase-shift database, as well as to low-energy scattering parameters and deuteron properties, the Argonne v_{18} potential provides an accurate description of scattering data by construction.

The three-nucleon potential V_{ijk}, whose inclusion is needed to reproduce the observed binding energies of the three-nucleon system and the empirical nuclear matter equilibrium properties, consists of the Fujita-Miyazawa two-pion exchange potential supplemented by a purely phenomenological repulsive contribution [12].

The predictive power of the dynamical model based on the Hamiltonian of Eq. (1) has been extensively tested by computing the energies of the ground and low-lying excited states of nuclei with $A \leqslant 12$. The results of these studies, in which the many-body Schrödinger equation is solved *exactly* using stochastic methods, turn out to be in excellent agreement with experimental data [13]. Accurate calculations can also be carried out for uniform nuclear matter, exploiting translational invariance and using the stochastic method [14], the variational approach [15], or G-matrix perturbation theory [16,17].

One of the most prominent features of the NN potential is the strongly repulsive core, whose cleanest manifestation is the observed saturation of nuclear charge densities. Owing to the presence of the core, the NN potential cannot be used to carry out *ab initio* microscopic calculations of nuclear observables using standard perturbation theory. The matrix elements of the interaction Hamiltonian between eigenstates of the noninteracting system, Fermi gas states in the case of uniform nuclear matter, turn out to be very large or even divergent.

In the G-matrix approach this problem is circumvented by replacing the bare NN potential with the *well-behaved* operator G, defined through the Bethe-Goldstone equation,

$$\begin{aligned}\langle ij|G(E)|kl\rangle &= G_{ij,kl}(E) \\ &= v_{ij,kl} + \sum_{mn} v_{ij,mn} \frac{Q_{mn}}{E - \epsilon_m - \epsilon_n + i\eta} \\ &\quad \times G_{mn,kl}(E), \end{aligned} \tag{5}$$

where $i \equiv (\mathbf{k}_i, s_i, t_i)$, with $\mathbf{k}_i$, s_i and t_i being the momentum and the spin and isospin projections specifying the ith single-particle state. The Pauli operator Q_{mn} restricts the sum over intermediate states to those compatible with the exclusion principle, while the so-called starting energy E corresponds to the sum of the nonrelativistic energies of the interacting nucleons.

The single-particle energy of a nucleon in state i is given by

$$\epsilon_i = \frac{k_i^2}{2m} + \mathrm{Re}[U_i], \tag{6}$$

where U_i describes the mean field felt by the nucleon owing to its interactions with the other particles of the medium. In the so-called Brueckner-Hartree-Fock approximation, U_i is calculated in the "on-shell approximation" through a self-consistent process. The resulting expression is

$$U_i = \sum_{j\in\{F\}} \langle ij|G(E = \epsilon_i + \epsilon_j)|ij\rangle_a, \tag{7}$$

where the sum runs over all occupied states in the Fermi sea $\{F\}$ and the two-nucleon matrix elements are properly antisymmetrized. We note here that the so-called continuous prescription [17] has been adopted for the single-particle potential when solving the Bethe-Goldstone equation. As shown in Ref. [18], the contribution to the energy per particle from three-hole line diagrams is minimized by this prescription.

Once a self-consistent solution of the G matrix is achieved, the energy per particle at the two-hole line level takes the form

$$\frac{E}{A} = \frac{3}{5}\frac{k_F^2}{2m} + \frac{1}{2}\sum_{i,j\in\{F\}} \langle ij|G(E = \epsilon_i + \epsilon_j)|ij\rangle_a, \tag{8}$$

where k_F is the Fermi momentum, related to the density through the relation $\rho = \nu k_F^3/6\pi^2$, ν being the spin-isospin degeneracy of the momentum eigenstates ($\nu = 2$ and $\nu = 4$ for pure neutron matter and symmetric nuclear matter, respectively).

In the approach based on correlated wave functions one uses the bare potential v, whose nonperturbative effects are incorporated in the basis states, obtained from the Fermi gas states $|n_{\mathrm{FG}}\rangle$ through the transformation

$$|n\rangle = F|n_{\mathrm{FG}}\rangle. \tag{9}$$

The operator F, embodying the correlation structure induced by the NN interaction, is written in the form

$$F = \mathcal{S}\prod_{ij} f_{ij}, \tag{10}$$

where $\mathcal{S}$ is the symmetrization operator accounting for the fact that, in general, $[f_{ij}, f_{ik}] \neq 0$. The two-body correlation functions f_{ij}, whose operator structure reflects the complexity of the NN potential, are written in the form

$$f_{ij} = \sum_{n=1}^{6} f^n(r_{ij}) O_{ij}^n, \tag{11}$$

with the O_{ij}^n given by Eq. (3).

The shapes of the radial functions $f^n(r_{ij})$ are determined through functional minimization of the expectation value of the nuclear Hamiltonian in the correlated ground state, carried out at the two-body level of the cluster expansion [19]. The resulting Euler Lagrange equations have been solved using correlation ranges taken from Ref. [20].

Within the CBF approach, at the two-body cluster level, one finds [9,10]

$$\frac{E}{A} = \frac{3}{5}\frac{k_F^2}{2m} + \sum_{j>i}\langle ij|V_{\mathrm{eff}}|ij\rangle_a, \tag{12}$$

where

$$V_{\mathrm{eff}} = \sum_{i<j} f_{ij}^\dagger \left[-\frac{1}{m}(\nabla^2 f_{ij}) - \frac{2}{m}(\boldsymbol{\nabla} f_{ij})\cdot\boldsymbol{\nabla} + v_{ij} f_{ij} \right], \tag{13}$$

and the derivatives act on the relative coordinates.

The contributions of many-body clusters, not included in the effective interaction of Eq. (13), are expected to become important in the high-density regime relevant to neutron stars. In Ref. [10] the NN potential has been modified to effectively take into account processes involving more than two nucleons. The resulting binding energies of both symmetric nuclear matter and pure neutron matter turn out to be in fairly good agreement with those obtained in Ref. [15] using the FHNC approach and the full Argonne v_{18} potential over a broad density range.

One would be tempted to exploit the analogies between Eq. (8) and Eq. (12), to establish a direct link between G and $V_{\rm eff}$. Hovewer, determining such a connection at the operator level is not trivial. To see this, just consider that, while all matrix elements of G involve the bare interaction v only, the matrix elements of $V_{\rm eff}$ also include purely kinetic contributions, not containing v, which arise from the derivatives of the correlation functions. In addition, unlike $V_{\rm eff}$, G exhibits an explicit energy dependence.

The CBF effective interaction, being defined through its ground-state expectation value, is somewhat limited in scope, with respect to the G-matrix effective interaction. However, a systematic comparison between the two formalisms can be carried out at the level of matrix elements. In this work we focus on the matrix elements of the effective interactions in momentum space relevant to calculation of the NN scattering rate in pure neutron matter, whose knowledge is required to obtain the transport coefficients within the Landau-Abrikosov-Khalatnikov formalism.

We have used the truncated version of the Argonne v_{18} potential referred to as v_6' [21], whose definition only involves the static contributions, that is, those corresponding to $n \leqslant 6$, in Eq. (3). The CBF effective interaction derived from this potential has also been used to obtain a weak response of nuclear matter at moderate momentum transfer [9,22].

For the sake of simplicity, in this work we have neglected the contribution of the three-nucleon potential appearing in Eq. (1).

III. NUCLEON-NUCLEON SCATTERING IN THE NUCLEAR MEDIUM

A. Kinematics

Consider the process in which two nucleons carrying momenta $\mathbf{k}_1$ and $\mathbf{k}_2$ scatter to final states of momenta $\mathbf{k}_1'$ and $\mathbf{k}_2'$. The total energy of the initial state,

$$E = \frac{\mathbf{k}_1^2}{2m} + \frac{\mathbf{k}_2^2}{2m}, \tag{14}$$

can be conveniently rewritten in terms of the center of mass (c.m.) and relative momenta, $\mathbf{K} = \mathbf{k}_1 + \mathbf{k}_2$ and $\mathbf{k} = (\mathbf{k}_1 - \mathbf{k}_2)/2$, as

$$E = \frac{\mathbf{K}^2}{2M} + \frac{\mathbf{k}^2}{2\mu} = \mathcal{E} + \mathcal{E}_{\rm rel}, \tag{15}$$

with $M = 2m$ and $\mu = m/2$.

In the reference frame in which the c.m. of the system is at rest (c.m. frame) $E = E_{\rm c.m.} = \mathcal{E}_{\rm rel}$, while in the laboratory (L) frame, in which $\mathbf{k}_2 = 0$, $E = E_{\rm L} = 2\mathcal{E}_{\rm rel}$.

Analysis of the NN scattering rates relevant to the calculation of transport coefficients is carried out in the frame in which the Fermi sphere is at rest, often referred to as the AK frame. Moreover, in the low-temperature regime, in which the results of Ref. [3] are applicable, scattering processes can only involve nucleons with momenta close to the Fermi momentum. Therefore, one can set

$$|\mathbf{k}_1| = |\mathbf{k}_2| = |\mathbf{k}_1'| = |\mathbf{k}_2'| = k_F. \tag{16}$$

At energies below the pion production threshold the scattering process is elastic, so that the requirement of energy conservation,

$$\begin{aligned}(\mathbf{k}_1 + \mathbf{k}_2)^2 &= 2k_F^2(1 + \cos\theta) \\ &= (\mathbf{k}_1' + \mathbf{k}_2')^2 = 2k_F^2(1 + \cos\theta'),\end{aligned} \tag{17}$$

implies that the angle between the momenta of the two nucleons is the same before and after the collision. In general, however, the angle ϕ between the initial and the final relative momenta, $\mathbf{k}$ and $\mathbf{k}' = (\mathbf{k}_1' - \mathbf{k}_2')/2$, defined through

$$\cos\phi = \frac{(\mathbf{k}\cdot\mathbf{k}')}{|\mathbf{k}||\mathbf{k}'|}, \tag{18}$$

does not vanish. Hence, for any given Fermi momentum, that is, for any given matter density, the scattering process in the AK frame is specified by the c.m. energy,

$$\mathcal{E}_{\rm AK} = \frac{k_F^2}{2m}(1 + \cos\theta), \tag{19}$$

and the two angles θ and ϕ.

As the NN scattering cross section is often evaluated in the c.m. frame, it is convenient to establish a relationship between kinematical variables in the c.m. frame and those in the AK frame. Exploiting the frame invariance of the relative energy, we easily obtain

$$E_{\rm c.m.} = \frac{k_F^2}{2m}(1 - \cos\theta), \tag{20}$$

while the c.m. scattering angle $\theta_{\rm c.m.}$ can be indentified with ϕ, defined in Eq. (18).

B. Cross section

In both the G-matrix and the CBF efffective interaction approaches, the NN cross section in matter at density ρ can be written in the form

$$\frac{d\sigma}{d\Omega_{\mathbf{k}'}} = \frac{m^{\star 2}}{16\pi^2}\sum_{SMM'}\left|\mathcal{M}_S^{MM'}(\theta,\phi)\right|^2, \tag{21}$$

where $m^\star$ is the nucleon effective mass, and the transition amplitude in the channel of total spin S and initial and final spin projections M and M', $\mathcal{M}_S^{MM'}(\theta,\phi)$, involves the matrix elements of either G or $V_{\rm eff}$ between Fermi gas states.

Numerical calculations of the cross sections are carried out, expanding $\mathcal{M}_S^{MM'}(\theta,\phi)$ in partial waves. In the case of pure neutron matter, in which the total isospin of the interacting pair

is $T = 1$, the expansion only involves partial waves of even (odd) angular momentum in spin singlet (triplet) states.

The matrix elements of the CBF effective interaction can be written in the form

$$M^{SJ}_{\ell\ell'}(k) = \frac{2}{\pi}\int r^2 dr\, j_\ell(kr)\langle \ell' SJ|V_{\rm eff}|\ell SJ\rangle\, j_{\ell'}(kr). \qquad (22)$$

In this equation, ℓ and J denote the orbital and total angular momentum, respectively, j_ℓ is the spherical Bessel function, $|\ell SJ\rangle$ is the spin-angle state, and r is the magnitude of the relative distance. Note that, owing to the presence of the tensor operator of Eq. (4), the NN potential couples states of different orbital angular momenta. These matrix elements are directly comparable with those obtained from the partial wave expansion of the G matrix [see Eq. (5)].

In Fig. 1 we show the matrix element $M(^1S_0) = M^{00}_{00}$, evaluated at nuclear matter equilibrium density, $\rho_0 = 0.16$ fm^{-3} (top), and $2\rho_0$ (bottom), in the kinematical setup described in Sec. III A. The solid and dashed lines correspond to the matrix elements of the CBF and G-matrix effective interactions, respectively, while the dot-dashed line was obtained by replacing $V_{\rm eff}$ with the bare v'_6 potential. Renormalization of the NN interaction, carried out by either solving the Bethe-Goldstone equation or modifying the basis states, appears to have a strong impact on the matrix elements, which become more attractive with respect to the matrix elements of the bare interaction. On the other hand, the CBF and G-matrix approaches yield

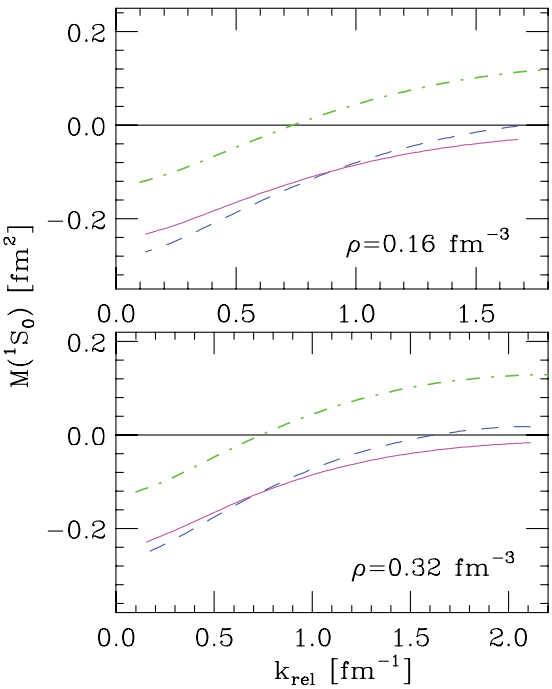

FIG. 1. (Color online) Top: $M(^1S_0)$ matrix element of the CBF [solid (pink) line] and G-matrix [dashed (blue) line] effective interactions [M^{00}_{00} in Eq. (22)] for neutron matter at nuclear matter equilibrium density, as a function of relative momentum. For comparison, the dot-dashed (green) line shows the result corresponding to the bare v'_6 potential. Bottom: Same as the top panel, but for density $\rho = 2\rho_0$.

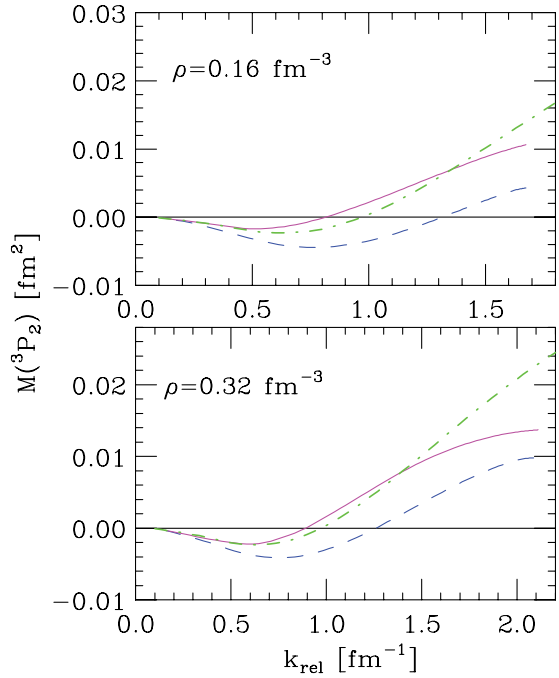

FIG. 2. (Color online) Same as Fig. 1, but for the $M(^3P_2)$ matrix elements.

rather similar results in the considered range of densities and momenta.

The matrix elements $M(^3P_2) = M^{12}_{11}$ are shown in Fig. 2. It appears that in this channel the results obtained using the CBF are closer to those corresponding to the bare interaction, while being appreciably different from the G-matrix results. Note, however, that the matrix elements corresponding to the $^3P_2$ channel are over one order of magnitude smaller than those corresponding to the $^1S_0$ channel.

It must be pointed out that the density dependence of the matrix elements is rather mild. In the CBF approach the density dependence arises from the two-body correlation functions, while in the G-matrix it comes through the presence of the Pauli operator and the single-particle potentials appearing in the denominator of Eq. (5). In addition, one should also take into account the density dependence associated with the starting energy E, as the matrix elements reported in Figs. 1 and 2 were computed at twice the Fermi energy of the corresponding density.

The convergence of the partial-wave expansion is illustrated in Fig. 3, showing the ratio

$$R_L = \frac{1}{\sigma_{\rm tot}}\sum_{\ell=0}^{L}\sigma^\ell_{\rm tot} \qquad (23)$$

as a function of the c.m. energy [see Eq. (20)]. In Eq. (23) $\sigma_{\rm tot}$ is the total in-medium NN cross section, while $\sigma^\ell_{\rm tot}$ denotes the contribution of the ℓth partial wave. All cross sections were evaluated in the kinematical setup relevant to the calculation of transport coefficients, discussed in Sec. III A. The definition obviously implies that, as $L \to \infty$, $R_L \to 1$.

The results in Fig. 3 show that the total cross section obtained including only the partial waves with $\ell = 0$ and 1,

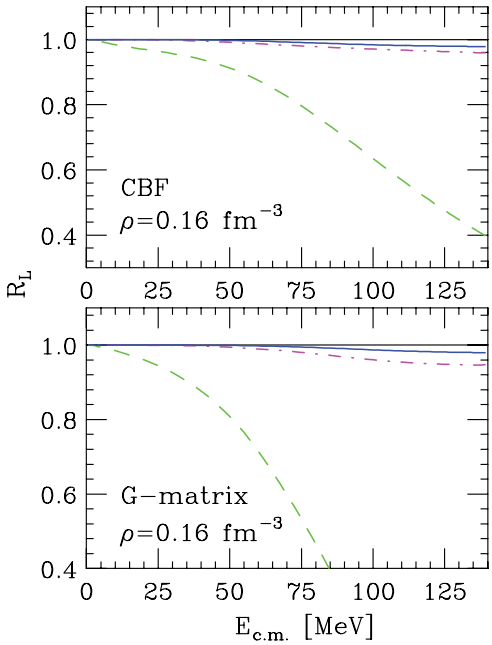

FIG. 3. (Color online) Energy dependence of the ratio R_L, defined by Eq. (23). The dashed (green), dot-dashed (pink), and solid (blue) lines were obtained including the contributions of states of angluar momentum ℓ up to 0, 1, and 2. The top and bottom panels correspond to CBF and G-matrix effective interactions, respectively.

corresponding to the spin-singlet and spin-triplet states of lowest angular momentum, is within less than 5% of the fully converged result. Comparison between the top and the bottom panels, corresponding to CBF and G-matrix effective interactions, also shows that the two approaches lead to a similar qualitative behavior, although the G-matrix R_0 exhibits a somewhat steeper energy dependence.

In Fig. 4 we compare the total NN cross section at nuclear matter equilibrium density, computed in the kinematics of Sec. III A, as a function of $E_{\rm c.m.}$. The difference in the cross sections obtained using the CBF (solid line) versus the G-matrix (dashed line) approaches does not exceed ∼20% at $E_{\rm c.m.} > 10$ MeV. On the other hand, the screening effect owing to the presence of the nuclear medium, illustrated by the difference between the solid and dashed lines and the dot-dashed line, corresponding to the free-space cross section obtained from the t matrix associated with the v_6' potential, turns out to be large. At $E_{\rm c.m.} > 100$ MeV, where the CBF and G-matrix results are very close to one another, the in-medium cross section turns out to be quenched by a factor of ∼3.

IV. TRANSPORT COEFFICIENTS

A. Abrikosov-Khalatnikov formalism

The theoretical description of transport properties of normal Fermi liquids is based on Landau theory [4]. Working within this framework and including the leading term in the low-temperature expansion, AK [3] obtained approximate expressions for the shear viscosity and the thermal conductivity. Let

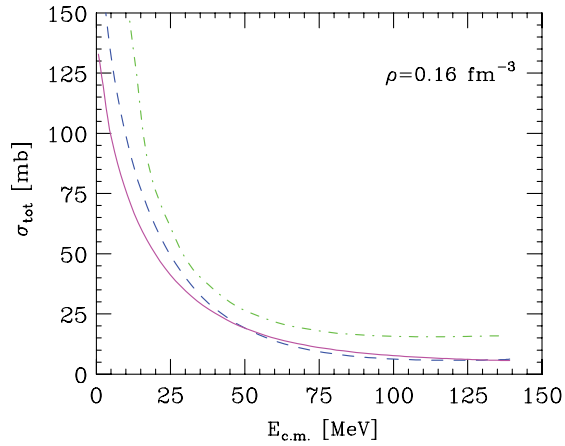

FIG. 4. (Color online) Total in-medium neutron-neutron cross section in neutron matter, computed at nuclear matter equilibrium density as a function of energy in the center-of-mass frame. The solid (pink) and dashed (blue) lines were obtained using the CBF and G-matrix effective interactions, respectively, in the kinematical setup discussed in Sec. III A. For comparison, the dot-dashed (green) line shows the free-space cross section, obtained from the t matrix associated with the v_6' potential.

us consider viscosity, as an example. The AK result reads

$$\eta_{\rm AK} = \frac{1}{5}\rho m^\star v_F^2 \tau \frac{2}{\pi^2(1-\lambda_\eta)}, \tag{24}$$

where $v_F = k_F/m^\star$ is the Fermi velocity, and $m^\star$ and τ denote the quasiparticle effective mass and lifetime, respectively. The latter can be written in terms of the angle-averaged scattering probability $\langle \mathcal{W} \rangle$, with [see Eq. (21)]

$$\mathcal{W}(\theta,\phi) = \sum_{SMM'} \left|\mathcal{M}_S^{MM'}(\theta,\phi)\right|^2, \tag{25}$$

according to

$$\tau T^2 = \frac{8\pi^4}{m^{*3}} \frac{1}{\langle \mathcal{W} \rangle}, \tag{26}$$

where T is the temperature and

$$\langle \mathcal{W} \rangle = \int \frac{d\Omega}{2\pi} \frac{\mathcal{W}(\theta,\phi)}{\cos(\theta/2)}. \tag{27}$$

Note that, as pointed out in Sec. III A, the scattering process involves quasiparticles on the Fermi surface. As a consequence, for any given density ρ, $\mathcal{W}$ depends only on the angular variables θ and ϕ. Finally, the quantity λ_η appearing in Eq. (24) is defined as

$$\lambda_\eta = \frac{\langle \mathcal{W}[1 - 3\sin^4(\theta/2)\sin^2\phi] \rangle}{\langle \mathcal{W} \rangle}. \tag{28}$$

The exact solution of the equation derived in Ref. [3], obtained by Brooker and Sykes [23], reads

$$\eta = \eta_{\rm AK} \frac{1-\lambda_\eta}{4} \times \sum_{k=0}^{\infty} \frac{4k+3}{(k+1)(2k+1)[(k+1)(2k+1)-\lambda_\eta]}, \tag{29}$$

the size of the correction with respect to the result of Eq. (24) being $0.750 < (\eta/\eta_{\rm AK}) < 0.925$.

The expression of the thermal conductivity κ is obtained following the same procedure, the only difference being that in this case the leading term in the low-energy expansion is linear, rather than quadratic, in the inverse temperature T^{-1}. The resulting expression is

$$\kappa = \kappa_{\rm AK}\frac{3-\lambda_\kappa}{4} \times \sum_{k=0}^{\infty}\frac{4k+5}{(k+1)(2k+3)[(k+1)(2k+3)-\lambda_\kappa]}, \quad (30)$$

where

$$\kappa_{\rm AK} = \frac{1}{T}\,\frac{8}{3}\,\frac{k_F^3}{m^{\star 4}}\,\frac{2\pi^2}{\langle\mathcal{W}\rangle(3-\lambda_\kappa)}, \quad (31)$$

and

$$\lambda_\kappa = \frac{\langle\mathcal{W}(1+2\cos\theta)\rangle}{\langle\mathcal{W}\rangle}. \quad (32)$$

In this case the correction to the AK result turns out to be larger. From Eq. (32) it follows that $-1 < \lambda_\kappa < 3$, in turn implying [see Eq. (30)] $0.417 < (\kappa/\kappa_{\rm AK}) < 0.561$.

B. Results

Figures 5 and 6 show the T-independent quantities ηT^2 and κT, respectively, as a function of density. The calculations were carried out using the formalism described in the previous section and the scattering probabilities $\mathcal{W}(\theta,\phi)$ obtained from both the G-matrix and the CBF effective interactions, which were computed at zero temperature. For comparison, in Fig. 5 we also display, by the dot-dashed line, the results obtained from the free-space scattering probability, computed using the t matrix associated with the bare v_6' potential.

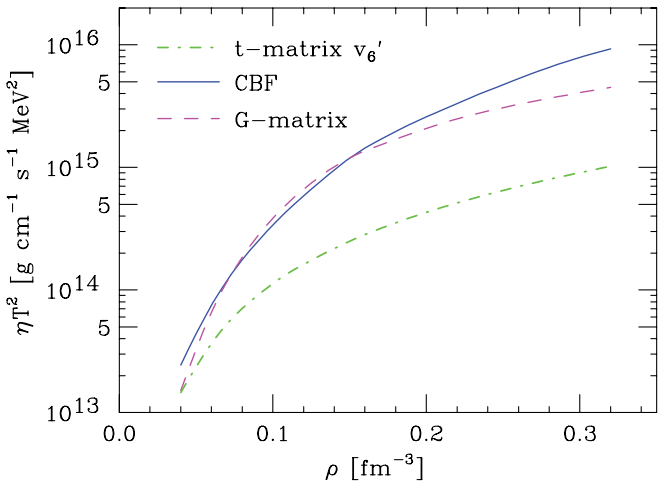

FIG. 5. (Color online) Density dependence of the T-independent quantity ηT^2 in pure neutron matter. The solid (blue) and dashed (pink) lines correspond to the CBF and G-matrix effective interactions, respectively, while the dot-dashed (green) line shows the results obtained from the t matrix associated with the v_6' potential.

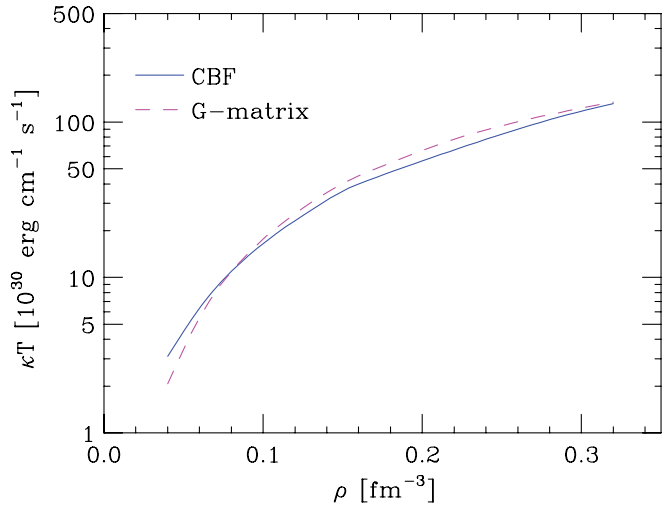

FIG. 6. (Color online) Density dependence of the T-independent quantity κT in pure neutron matter. The solid (blue) and dashed (pink) lines were obtained using the CBF and G-matrix effective interactions, respectively.

As the ratios $m^\star/m$ resulting from the two approaches, CBF and G matrix, turn out to be rather close to one another (the difference never exceeds a few percent in the density range shown in Figs. 5 and 6), all calculations were carried out using the CBF effective masses.

Figure 5 clearly indicates that medium modifications of the NN scattering cross sections play a critical role, leading to a dramatic enhancement of the viscosity. A similar effect is observed in the case of thermal conductivity [24].

Comparison between Figs. 5 and 6 shows that, while the density dependence of the thermal conductivity resulting from the two approaches looks remarkably similar, in the case of viscosity, sizable discrepancies occur at densities higher than the nuclear matter equilibrium density.

This feature can be easily explained considering the different angular dependence of the integrands in Eqs. (28) and (32), which determine the functions λ_η and λ_κ, respectively. In the case of λ_κ, $\mathcal{W}(\theta,\phi)$ is weighted with a function that depends only on θ. As a consequence, the result depends only on the ϕ-integrated scattering probability, which is trivially related to the *total* cross section [see Eq. (21)] at energy $E_{\rm c.m.}$ given by Eq. (20). Hence, the similar behavior exhibited by the two curves in Fig. 6 merely reflects the fact that the total cross sections obtained from the G-matrix and CBF approaches turn out to be close to one another (see Fig. 4). On the other hand, on the right-hand side of Eq. (28) the scattering probability is weighted with a factor that emphasizes the differences in the ϕ dependence of the CBF and G-matrix $\mathcal{W}(\theta,\phi)$.

We have verified that the large discrepancy between the solid and the dashed curves in Fig. 5 at high density is in fact ascribable to λ_η. The λ_η-independent quantities $\eta_{\rm AK}(1-\lambda_\eta)/4$ obtained from the CBF and G-matrix approaches turn out to be within less than 5% of one another at $\rho = 0.32$ fm^{-3}. On the other hand, removal of the λ_κ dependence in $\kappa_{\rm AK}$ does not produce any significant effects.

V. CONCLUSIONS

Many-body theory provides a fully consistent framework suited to construct effective interactions starting from highly realistic models of nuclear dynamics. In this work, we have employed the effective interactions resulting from the G-matrix and CBF approaches to compute the in-medium NN cross sections, which are needed to obtain the transport coefficient within the Landau-Abrikosov-Khalatnikov formalism.

The calculations have been carried out using the truncated v_6' form of the NN potential from Ref. [11]. The effects of three- and many-body forces, though known to be sizable at high density, have not been taken into account. The results in Ref. [10] show that many-body forces give rise to a change in the shear viscosity of less than 10% at $\rho \lesssim 0.32$ fm^{-3}. Hence, their inclusion is not likely to significantly affect the main conclusions of our work.

The approach based on effective interactions allows one to consistently take into account screening effects arising from short-range NN correlations, which lead to a large decrease in the scattering cross section. As a consequence, the shear viscosity and thermal conductivity obtained from the effective interactions turn out to be much larger than the corresponding quantities computed using the bare NN potential.

Our work, showing that the results of the G-matrix and CBF schemes are in reasonable agreement with one another, suggests that as long as the effective interaction is based on a *realistic* NN potential, strongly constrained by the large data set of NN scattering phase shifts, the model dependence associated with the many-body approach employed is not critical.

The additional model dependence associated with the choice of a specific NN potential, mainly owing to differences in the off-shell behavior of the tensor force, is not expected to be large. This effect was recently estimated in Ref. [25], whose authors computed the in-medium NN cross sections within the Dirac-Brueckner-Hartree-Fock approach using the Bonn A, B, and C potentials. The resulting total cross sections turn out to be quite similar, their spread at $\rho \sim 2\rho_0$ and $E_{\text{c.m.}} \sim 100$ MeV being $\lesssim 4\%$ [25].

On the other hand, it must be pointed out that Skyrme effective interactions (for a recent and comprehensive discussion of the application of the Skyrme approach to nuclear matter and neutron stars, see Ref. [26]), mainly constructed by fitting bulk properties of nuclear matter, predict in-medium NN cross sections whose behavior is significantly different from that predicted by the G-matrix and CBF effective interactions. As a result, the values of the viscosity and thermal conductivity coefficients computed using Skyrme effective interactions turn out to be much lower than those shown in Figs. 5 and 6. For example, using the SLya effective interaction, adjusted to reproduce the microscopically derived EOS of neutron and nuclear matter [27], one finds at nuclear matter equilibrium density $\eta T^2 \sim 6 \times 10^{13}$ g cm^{-1} s^{-1} MeV^2 and $\kappa T \sim 4 \times 10^{30}$ erg cm^{-1} s^{-1}, compared to $\sim 1.4 \times 10^{15}$ g cm^{-1} s^{-1} MeV^2 and $\kappa T \sim 4 \times 10^{31}$ erg cm^{-1} s^{-1} obtained from the G-matrix and CBF formalisms. While the Skyrme approach has proved to be very useful in many contexts, these results suggest that the determination of the transport properties of nuclear matter requires effective interactions providing a quantitative account of the observed NN scattering data in the limit of vanishing density.

ACKNOWLEDGMENTS

M.V. gratefully acknowledges the hospitality of the Departament d'Estructura i Constituents de la Matèria, Barcelona. This work was partially supported by FEDER/FCT (Project No. CERN/FP/83505/2008), Consolider-Ingenio 2010 (programma CPAN CSD2007-00042 and Grant No. FIS2008-01661), MEC/FEDER (Project No. 2009SGR-1289), and the European Science Foundation research networking program COMPSTAR.

[1] N. Anderson and K. D. Kokkotas, Int. J. Mod. Phys. D **10**, 381 (2001).
[2] D. G. Yakovlev, A. D. Kaminker, O. Y. Gnedin, and P. Haensel, Phys. Rep. **354**, 1 (2001).
[3] A. A. Abrikosov and I. M. Khalatnikov, Sov. Phys. JETP **5**, 887 (1957); Rep. Prog. Phys. **22**, 329 (1959).
[4] G. Baym and C. Pethick, *Landau Fermi-Liquid Theory* (John Wiley & Sons, New York, 1991).
[5] E. Flowers and N. Itoh, Astrophys. J. **206**, 218 (1976).
[6] E. Flowers and N. Itoh, Astrophys. J. **230**, 847 (1979).
[7] D. A. Baiko and P. Haensel, Acta Phys. Pol. B **30**, 1097 (1999).
[8] J. Wambach, T. L. Aisworth, and D. Pines, Nucl. Phys. **555**, 128 (1993).
[9] S. Cowell and V. R. Pandharipande, Phys. Rev. C **73**, 025801 (2006).
[10] O. Benhar and M. Valli, Phys. Rev. Lett. **99**, 232501 (2007).
[11] R. B. Wiringa, V. G. J. Stoks, and R. Schiavilla, Phys. Rev. C **51**, 38 (1995).
[12] B. S. Pudliner, V. R. Pandharipande, J. Carlson, and R. B. Wiringa, Phys. Rev. Lett. **74**, 4396 (1995).
[13] S. C. Pieper and R. B. Wiringa, Annu. Rev. Nucl. Part. Sci. **51**, 53 (2001).
[14] A. Sarsa, S. Fantoni, K. E. Schmidt, and F. Pederiva, Phys. Rev. C **68**, 024308 (2003).
[15] A. Akmal, V. R. Pandharipande, and D. G Ravenhall, Phys. Rev. C **58**, 1804 (1998).
[16] H. Müther and A. Polls, Prog. Part. Nucl. Phys. **45**, 243 (2000).
[17] M. Baldo, in *Nuclear Methods and the Nuclear Equation of State*, edited by M. Baldo, International Review of Nuclear Physics, Vol. 8 (World Scientific, Singapore, 1999).
[18] H. Q. Song, M. Baldo, G. Giansiracusa, and U. Lombardo, Phys. Rev. Lett. **81**, 1584 (1998).
[19] R. B. Wiringa and V. R. Pandharipande, Phys. Lett. **B99**, 1 (1981).
[20] A. Akmal, Ph.D. thesis, University of Illinois at Urbana Champaign, 1998.

[21] B. S. Pudliner, V. R. Pandharipande, J. Carlson, S. C. Pieper, and R. B. Wiringa, Phys. Rev. C **56**, 1720 (1997).
[22] O. Benhar and N. Farina, Phys. Lett. **B680**, 305 (2009).
[23] G. A. Brooker and J. Sykes, Phys. Rev. Lett. **21**, 279 (1968).
[24] O. Benhar, N. Farina, S. Fiorilla, and M. Valli, AIP Conf. Proc. **1056**, 248 (2008).
[25] H. F. Zhang, Z. H. Li, U. Lombardo, P. Y. Luo, F. Sammarruca, and W. Zuo, Phys. Rev. C **76**, 054001 (2007).
[26] J. R. Stone, J. C. Miller, R. Koncewicz, P. D. Stevenson, and M. R. Strayer, Phys. Rev. C **68**, 034324 (2003).
[27] E. Chabanat, P. Bonche, P. Haensel, J. Meyer, and R. Schaeffer, Nucl. Phys. **A627**, 710 (1997).